IEEE Open Access Journal of
Power and Energy

Received 24 April 2020; revised 21 July 2020 and 31 August 2020; accepted 3 October 2020. Date of publication 12 October 2020; date of current version 9 November 2020.

Digital Object Identifier 10.1109/OAJPE.2020.3030242

Asynchronous Economic Dispatch for Combined Heat and Power Systems

XIN QIN [1] (Student Member, IEEE), HONGBIN SUN [2] (Fellow, IEEE), AND YE GUO [1] (Senior Member, IEEE)

[1]Tsinghua–Berkeley Shenzhen Institute, Tsinghua University, Shenzhen 518055, China
[2]Department of Electrical Engineering, Tsinghua University, Beijing 100084, China

CORRESPONDING AUTHOR: H. SUN (shb@mail.tsinghua.edu.cn)

This work was supported by the National Natural Science Foundation of China (NSFC) under Grant 51537006.

ABSTRACT In the day-ahead economic dispatch of combined heat and power systems, the electric power system is adjusted in minutes because of the short dynamic time and the requirement of real-time power balance, while the heating system is dispatched in hours due to its large inertia and long dynamic process. However, the different dispatch time scales of electricity and heat are ignored by existing synchronous dispatch methods, which limits the improvement of system efficiency. To address this challenge, in this article, the asynchronous dispatch method is proposed and instantiated by two different dispatch models featuring a short electric dispatch time scale and a long heat dispatch time scale. Case studies demonstrate the asynchronous dispatch method can overcome the efficiency and reliability problems caused by the existing synchronous dispatch methods.

INDEX TERMS Combined heat and power system, different time scales, economic dispatch, dispatch interval.

NOMENCLATURE

A. ABBREVIATIONS

CHP	Combined heat and power.
DC	Direct current.

B. SETS

E	Set of electric buses.
G	Set of energy sources.
H	Set of heat nodes.
H_G/H_L	Set of heat source/load nodes.
$In(i)/Lv(i)$	Sets of pipelines injecting into/leaving from node i.
L	Set of electric power lines.
P_s/P_r	Sets of pipelines in the heat supply/return networks.
W_k	Set of electric time periods within the corresponding heat time period k.

C. PARAMETERS AND FUNCTIONS

A_i	Cross-sectional area of pipeline i.
$B_{k,i}/K_{k,i}/v_{k,i}$	Coefficients of the kth boundary of the feasible operating region of CHP unit at energy source i.
c_p	Heat capacity of water.
C_t^G	Electricity price at period t.
$CC_{i,t}(p_{i,t}, h_{i,t})$	Cost function of CHP unit at energy source i at period t which includes electric power terms.
$CC_{i,t}(h_{i,t})$	Cost function of CHP unit at energy source i at period t which does not include electric power terms.
$CG_{i,t}(p_{i,t})$	Cost function of electricity purchase from the grid at energy source i at period t.
$CT_{i,t}(p_{i,t})$	Cost function of thermal generator at energy source i at period t.
$d_{i,t}$	Electric load demand of bus i at period t.
$D_{e,i}/U_{e,i}$	Downward/upward electric ramping capacities of CHP unit at energy source i.
$D_{h,i}/U_{h,i}$	Downward/upward heat ramping capacities of CHP unit at energy source i.
k_E	An integer coefficient that describes the relationship between the electric and heat dispatch intervals.
$K_{i,t,k}$	kth coefficient defining the outlet temperature of pipeline i at period t.
$l_{i,t}/\bar{l}_{i,t}$	Lower/upper electric line power limits of line i at period t.
$m_{i,t}^n$	Node mass flow of node i at period t.
$m_{i,t}$	Pipe mass flow of pipeline i at period t.

$\underline{p}_i^G/\bar{p}_i^G$	Lower/upper limits of electricity purchase from the grid at energy source i.
$\underline{p}_i^T/\bar{p}_i^T$	Lower/upper limits of electric power output of thermal generator at energy source i.
$SF_{i,j}$	Shift factor of bus j to line i.
$\Delta t_E/\Delta t_H$	Electric/heat dispatch intervals in the hybrid model.
Δt	Dispatch interval in the identical model.
N_E/N_H	The last dispatch period in the electric power system/heating system in the hybrid model.
N	The last dispatch period in the identical model.
$T_{i,t}^a$	Ambient temperature of pipeline i at period t.
$T_{i,t}^{Set}$	Set temperature of energy source i at period t.
$\underline{T}_i^{NS}/\bar{T}_i^{NS}$	Lower/upper limits of exchanger supply temperature at node i.
$\underline{T}_i^{NR}/\bar{T}_i^{NR}$	Lower/upper limits of exchanger return temperature at node i.
λ_i	Thermal conductive coefficient of pipeline i.
ρ	Density of water.
$\eta_{i,t,j}^T/\eta_{i,t,j}^C$	jth cost coefficients of thermal generator/CHP unit at energy source i at period t.
$\gamma_{i,t}/\varphi_{i,t}$	Time delays coefficients of pipeline i at period t.
$\Gamma_G(i)$	Corresponding heat node of energy source i.

D. DECISION VARIABLES

$h_{i,t}^C$	Heat power output of CHP unit at energy source i at period t.
$h_{i,t}$	Heat power output of energy source i at period t.
$p_{i,t}^C/p_{i,t}^T/p_{i,t}^G$	Electric power outputs of CHP unit/thermal generator/tie-line power at energy source i at period t.
$p_{i,t}$	Electric power output of energy source i at period t.
$T_{i,t}^{NS}/T_{i,t}^{NR}$	Exchanger supply/return temperatures of node i at period t.
$T_{i,t}^S/T_{i,t}^R$	Temperatures of node i at period t in supply/return networks, after mixing.
$\tau_{i,t}^{SO}/\tau_{i,t}^{RO}$	Outlet temperatures of pipeline i at period t in heat supply/return networks.
$\tau_{i,t}^{\prime SO}/\tau_{i,t}^{\prime RO}$	Outlet temperatures without heat loss of pipeline i at period t in heat supply/return networks.
$\tau_{i,t}^{SI}/\tau_{i,t}^{RI}$	Inlet temperatures of pipeline i at period t in heat supply/return networks.

I. INTRODUCTION

A. BACKGROUND AND MOTIVATION

COMBINED heat and power systems have been deployed all over the world due to the high efficiency and low carbon emission [1], [2]. However, it is challenging to dispatch combined heat and power systems synchronously because it couples two energy systems with different time scales: With the requirement of real-time power balance, the electric power system is adjusted in minutes [3], whereas the heating system has much higher inertia and is usually adjusted in hours [4], [5].

Considering this different time scale characteristic, implementing the synchronous dispatch method, which dispatches the two energy systems with the same time scale, will lead to the dilemma of the time-scale selection: a shorter time scale will make the heating system difficult to dispatch effectively and a longer time scale cannot satisfy the real-time changing electric demand. Such a dilemma contradicts the motivation of deploying combined heat and power systems. Therefore, in this article, we propose the day-ahead asynchronous dispatch to incorporate the different dispatch time scales of electricity and heat.

B. RELATED WORKS

For clarity, the related research papers are summarized into 3 types as shown in Table 1, which are divided according to whether the different dispatch time scales and heat inertia are considered.

TABLE 1. Summary of existing research papers.

Type	Representative paper	Heating system inertia	Different dispatch time scales
1	[8]	×	×
2	[13][14]	√	×
3	[19][24]	Pending	√

The first type does not consider the heat dynamic process as well as the different time scales of electricity and heat. For example, papers [6]–[8] propose to operate the combined heat and power system following the electric dispatch time scale by assuming the heating system can reach steady-state in minutes. Although the inertia of the heat exchanger is considered, the dynamic process of the heating network is still neglected in [9]. Moreover, even for the short-term economic dispatch, the heating system is assumed to be adjusted as fast as the electric power system [10], [11]. Admittedly, ignoring the different time scales and heat inertia is an effective way to simplify the economic dispatch model. However, a part of dispatch commands may not be executed in practice because of the slow response of the heating system whose dynamic process varies from dozens minute to several hours [12].

As an improvement, the second type of research papers considers the heating system inertia, but it still ignores different dispatch time scales of electricity and heat. For instance, Li *et al.* [13], Lin *et al.* [14], and Yang *et al.* [15] use the heat pipeline inertia to accommodate more renewables. Building heat inertia is considered in [16] to provide additional flexibility. Also, some research papers adopt the variable mass flow to increase the system flexibility such as [17]. Unfortunately, these papers all assume the heating system can respond to

dispatch commands as fast as an electric power system, which may not be valid in reality.

To address the above problems in existing day-ahead synchronous dispatch methods, researchers propose hierarchical dispatch frameworks according to the adjustment time scales of different devices [19]–[23]. However, these research papers still use the synchronous method in each layer, which may leave power mismatches to the next dispatch layer. Recently, Gu *et al.* mentioned advantages of the asynchronous dispatch method which allows the different dispatch time scales of electricity and heat [24] in day-ahead economic dispatch. However, the optimization model and the necessity of using asynchronous are not addressed in [24].

C. KEY CONTRIBUTIONS

This article proposes the day-ahead asynchronous economic dispatch for combined heat and power systems, which incorporates different dispatch time scales of the electric power system and the heating system. The asynchronous dispatch method is instantiated by two models, a hybrid model and an identical model, where the hybrid model has higher calculation efficiency, and the identical model can be extended to deal with exceptional cases such as special dispatch intervals and multiple CHP units with different adjustment time scales.

This article also studies the factors influencing the performance of the asynchronous dispatch as well as drawbacks of the synchronous dispatch. In the case simulation, the influence of dispatch intervals on overall costs and calculation efficiency is studied. Then we use two cases to illustrate why the existing synchronous dispatch method either has problems in efficiency or fails to ensure reliability, which demonstrate the necessity of using the proposed asynchronous dispatch method.

D. ORGANIZATION OF THE PAPER

The remainder of this article is organized as follows. In Section II, the hybrid model for asynchronous dispatch is formulated. Section III presents the identical model to realize asynchronous dispatch. In Section IV, case studies demonstrate that the hybrid model and the identical model have the same solutions, and the influence of dispatch intervals is studied. Also, the advantages of using the asynchronous dispatch method are presented in Section IV.

II. HYBRID MODEL

As shown in Fig. 1, in the hybrid model, variables in the two energy systems have different time scales: The electric power system has a shorter dispatch interval Δt_E, while the heating system has a longer dispatch interval Δt_H. Generally, considering $N_E \geq N_H$, the constraints of the heating system are less than the electric power system.

A. OBJECTIVE FUNCTION

We assume an energy source may include a thermal generator, a CHP unit, and a tie-line connected to the main grid. For clarity, we use $p_{i,t} = p^G_{i,t} + p^T_{i,t} + p^C_{i,t}$ and $h_{i,t} = h^C_{i,t}$ to indicate

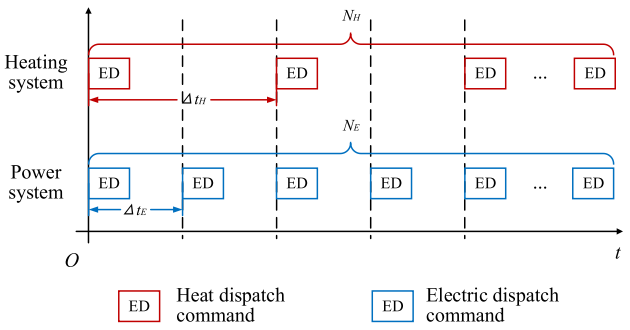

FIGURE 1. The illustration of dispatch commands in the hybrid model.

total electric and heat power outputs at energy source i. For example, if an energy source only has a thermal generator, then its $p^G_{i,t} = p^C_{i,t} = 0$, and $h_{i,t} = h^C_{i,t} = 0$.

The objective function of the hybrid model is to minimize the total generation costs of all energy sources at all time periods:

$$\begin{aligned}\min_{p^T_{i,t}, p^H_{i,t}, p^C_{i,t}, h^C_{i,t}} & f \\ = & \sum_{i\in G}\sum_{t=1}^{N_E}\left[CT_{i,t}(p^T_{i,t}) + CG_{i,t}(p^H_{i,t})\right]\Delta t_E \\ & + \sum_{i\in G}\left[\sum_{t=1}^{N_E} CC_{i,t}(p^C_{i,t}, h^C_{i,t})\Delta t_E + \sum_{t=1}^{N_H} CC_{i,t}(h^C_{i,t})\Delta t_H\right]\end{aligned} \tag{1}$$

The cost functions of thermal generators and CHP units at energy source i are expressed using quadratic functions of electricity and heat productions [17]:

$$CT_{i,t}(p^T_{i,t}) = \eta^T_{i,t,0} + \eta^T_{i,t,1} p^T_{I,T} + \eta^T_{i,t,3}\left(p^T_{i,t}\right)^2 \tag{2}$$

$$\begin{aligned}CC_{i,t} = & \underbrace{\eta^C_{i,t,0} + \eta^C_{i,t,1} p^C_{i,t} + \eta^C_{i,t,2}\left(p^C_{i,t}\right)^2 + \eta^C_{i,t,5} p^C_{i,t} h^C_{i,t}}_{CC_{i,t}(p^C_{i,t}, h^C_{i,t})} \\ & + \underbrace{\eta^C_{i,t,3} h^C_{i,t} + \eta^C_{i,t,4}\left(h^C_{i,t}\right)^2}_{CC_{i,t}(h^C_{i,t})}\end{aligned} \tag{3}$$

The cost function of the electricity purchase from the main grid is:

$$CG_{i,t}(p^G_{i,t}) = C^G_t p^G_{i,t} \tag{4}$$

B. ELECTRIC POWER SYSTEM CONSTRAINTS

In the electric power system, the DC power flow model is used. The real-time electric power balance is required between the generation side and the load side:

$$\sum_{i\in E} p_{i,t} = \sum_{i\in E} d_{i,t} \quad t = 1, 2, \ldots N_E \tag{5}$$

If a bus does not have an energy source, then its $p_{i,t} = 0$.

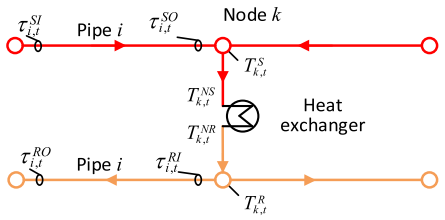

FIGURE 2. The physical model of the heating system.

The electric line power is calculated by:

$$l_{i,t} = \sum_{j \in E} SF_{i,j} \cdot (p_{j,t} - d_{j,t}) \forall i \in L, \quad t = 1, 2, \ldots N_E \tag{6}$$

The electric line power should be below its thermal limitation:

$$l_{i,t} \leq \sum_{j \in E} SF_{i,j} \cdot (p_{j,t} - d_{j,t}) \leq \bar{l}_{i,t} \forall i \in L, \quad t = 1, 2, \ldots N_E \tag{7}$$

C. HEATING SYSTEM CONSTRAINTS

In the heating system, we assume the medium is hot water, and the mass flow is the given value. These assumptions are widely adopted in the literature such as [13], [16], and [25].

The node gets heat power through the heat exchanger between the supply and return networks:

$$h_{i,t} = c_p m^n_{i,t} (T^{NS}_{i,t} - T^{NR}_{i,t}) \quad \forall i \in H, \quad t = 1, 2, \ldots N_H, \tag{8}$$

For clarity, the relationship between different heat variables is shown in the physical model in Fig. 2.

In the heat supply network, for load nodes $T^{NS}_{i,t} = T^{S}_{i,t}$. For source nodes $T^{S}_{i,t}$ is calculated using (12). Similarly, in the heat return network, for load nodes $T^{R}_{i,t}$ is calculated using (13). For source nodes $T^{NR}_{i,t} = T^{R}_{i,t}$.

To ensure the heat exchanger working conditions, the exchanger supply and return temperatures must satisfy:

$$\underline{T}^{NS}_{i} \leq T^{NS}_{i,t} \leq \bar{T}^{NS}_{i} \quad \forall i \in H, \quad t = 1, 2, \ldots N_H \tag{9}$$

$$\underline{T}^{NR}_{i} \leq T^{NR}_{i,t} \leq \bar{T}^{NR}_{i} \quad \forall i \in H, \quad t = 1, 2, \ldots N_H \tag{10}$$

To prevent the heat pipeline storage from being exhausted, the generated heat energy cannot be less than the load heat energy within scheduling periods:

$$\sum_{t=1}^{N_H} \left(\sum_{i \in H_G} h_{i,t} - \sum_{i \in H} h_{i,t} \right) \Delta t_H \geq 0 \tag{11}$$

The node temperature mixing equations are applied to calculate node temperature using the pipe outlet temperature:

$$\left(m^n_{i \in H_G, t} + \sum_j m_{j,t} \right) T^{S}_{i,t} = \left(m^n_{i \in H_G, t} T^{NS}_{i \in H_G, t} \right) + \left(\sum_j m_{j,t} \tau^{SO}_{j,t} \right) \quad \forall i \in H, j \in P_S \cap In(i), \quad t = 1, 2, \ldots N_H \tag{12}$$

$$\left(m^n_{i \in H_L, t} + \sum_j m_{j,t} \right) T^{R}_{i,t} = \left(m^n_{i \in H_L, t} T^{NR}_{i \in H_L, t} \right) + \left(\sum_j m_{j,t} \tau^{RO}_{j,t} \right) \quad \forall i \in H, j \in P_R \cap In(i), \quad t = 1, 2, \ldots N_H \tag{13}$$

The pipe inlet temperature equals the temperature of its connecting node:

$$\tau^{SI}_{j,t} = T^{S}_{i,t} j \in P_S \cap Lv(i), i \in H, \quad t = 1, 2, \ldots N_H \tag{14}$$

$$\tau^{RI}_{j,t} = T^{R}_{i,t} j \in P_R \cap Lv(i), i \in H, \quad t = 1, 2, \ldots N_H \tag{15}$$

The pipeline outlet temperature without loss is calculated by the method in [17]:

$$\tau'^{SO}_{i,t} = \sum_{k=t-\varphi_{i,t}}^{t-\gamma_{i,t}} K_{i,t,k} \tau^{SI}_{i,k} \forall i \in P_S, \quad t = 1, 2, \ldots N_H \tag{16}$$

$$\tau'^{RO}_{i,t} = \sum_{k=t-\varphi_{i,t}}^{t-\gamma_{i,t}} K_{i,t,k} \tau^{RI}_{i,k} \forall i \in P_R, \quad t = 1, 2, \ldots N_H \tag{17}$$

For the details of coefficient $K_{i,t,k}$ and integer intermediate coefficients $\gamma_{i,t}$ and $\varphi_{i,t}$, see [17].

Then the pipeline heat loss is considered:

$$\tau^{SO}_{i,t} = T^{a}_{i,t} + (\tau'^{SO}_{i,t} - T^{a}_{i,t}) \times \exp\left[-\frac{\lambda_i \Delta t_H}{A_i \rho c_p} \left(\gamma_{i,t} + \frac{1}{2} + \frac{S_{i,t} - R_{i,t}}{m_{i,t-\gamma_{i,t}} \Delta t_H} \right) \right] \forall i \in P_S, \quad t = 1, 2, \ldots N_H \tag{18}$$

$$\tau^{RO}_{i,t} = T^{a}_{i,t} + (\tau'^{RO}_{i,t} - T^{a}_{i,t}) \times \exp\left[-\frac{\lambda_i \Delta t_H}{A_i \rho c_p} \left(\gamma_{i,t} + \frac{1}{2} + \frac{S_{i,t} - R_{i,t}}{m_{i,t-\gamma_{i,t}} \Delta t_H} \right) \right] \forall i \in P_R, \quad t = 1, 2, \ldots N_H \tag{19}$$

D. ENERGY SOURCE CONSTRAINTS

1) COMBINED HEAT AND POWER UNITS

The feasible regions of different CHP units are shown in Fig. 3 (a) and (b) and described by polytopes in equation (20) and (21), respectively [13], [26]. Different from extraction condensing CHP units, the electric and heat power outputs of back-pressure units have a linear relationship.

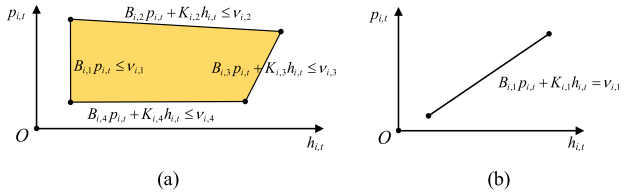

FIGURE 3. The feasible regions of the (a) extraction condensing and (b) back-pressure CHP unit.

Therefore, the electric power output of back-pressure units follows the time scale of the heating system:

$$B_{k,i}p_{i,t}^{C}+K_{k,i}h_{i,t}^{C}\le v_{k,i}\forall i\in G,\quad t=1,2,\ldots N_E \tag{20}$$

$$B_{k,i}p_{i,t}^{C}+K_{k,i}h_{i,t}^{C}=v_{k,i}\forall i\in G,\quad t=1,2,\ldots N_H \tag{21}$$

The ramping constraint indicates the increment or decrement of the source power outputs within a single period must not exceed the ramping capacity:

$$D_{e,i}\cdot\Delta t_E\le p_{i,t}^{C}-p_{i,t-1}^{C}\le U_{e,i}\cdot\Delta t_E\forall i\in G,\quad t=2,3,\ldots N_E \tag{22}$$

$$D_{h,i}\cdot\Delta t_H\le h_{i,t}^{C}-h_{i,t-1}^{C}\le U_{h,i}\cdot\Delta t_H\forall i\in G,\quad t=2,3,\ldots N_H \tag{23}$$

Moreover, the CHP unit supply temperature is usually set by operators:

$$T_{j,t}^{NS}=T_{i,t}^{Set}\forall i\in G, j=\Gamma_G(i),\quad t=1,2,\ldots N_H \tag{24}$$

2) THERMAL GENERATOR AND MAIN GRID

Since the thermal generator and the main grid do not generate heat, they follow the electric time scale. The electric power outputs of the thermal generator and the tie-line at energy source i must satisfy (25), while the thermal generator must satisfy ramping constraints (22).

$$\begin{aligned}\underline{p}_i^{G}&\le p_{i,t}^{G}\le\bar{p}_i^{G}\forall i\in G,\quad t=1,2,\ldots T_E\\ \underline{p}_i^{T}&\le p_{i,t}^{T}\le\bar{p}_i^{T}\forall i\in G,\quad t=1,2,\ldots T_E\end{aligned} \tag{25}$$

III. IDENTICAL MODEL

Another asynchronous dispatch model is called the identical model. As shown in Fig. 4, the two energy systems both adopt the electric dispatch interval, i.e., $\Delta t=\Delta t_E$.

To deal with the long dispatch time scale of the heating system, additional equality constraints (yellow blocks in Fig. 4) are added to guarantee the heat decision variables are invariant during each Δt_H. With these additional constraints, an asynchronous dispatch can be realized that satisfies the different adjustment abilities of the two energy systems. Compared with the hybrid model, the identical model has more constraints but the same solution, which is verified in case studies.

A. OBJECTIVE FUNCTION

The objective function of the identical model minimizes the total generation costs of all energy sources at all time

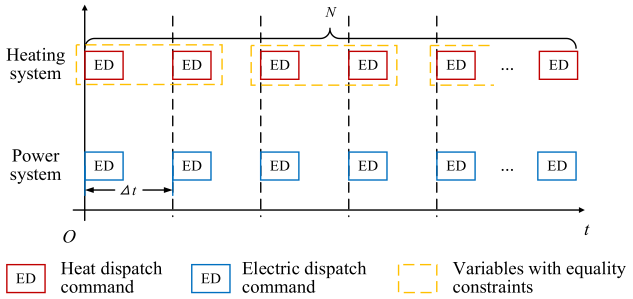

FIGURE 4. The illustration of dispatch commands in the identical model.

intervals:

$$\begin{aligned}&\min_{p_{i,t}^{T},p_{i,t}^{H},p_{i,t}^{C},h_{i,t}^{C}} f\\ &=\sum_{i\in G}\sum_{t=1}^{N}\left[CT_{i,t}(p_{i,t}^{T})+CG_{i,t}(p_{i,t}^{G})\right]\Delta t\\ &\quad+\sum_{i\in G}\sum_{t=1}^{N}\left[CC_{i,t}(p_{i,t}^{C},h_{i,t}^{C})+CC_{i,t}(h_{i,t}^{C})\right]\Delta t\end{aligned} \tag{26}$$

Substitute $\Delta t_H=k_E\cdot\Delta t_E=k_E\cdot\Delta t$ into (1), equation (26) equals (1). For special circumstances, see Appendix.

B. ELECTRIC POWER SYSTEM CONSTRAINTS

In the electric power system, the constraints of the identical model are the same as those in the hybrid model:

$$\sum_{i\in E}p_{i,t}=\sum_{i\in E}d_{i,t}t=1,2,\ldots N \tag{27}$$

$$l_{i,t}=\sum_{j\in E}SF_{i,j}\cdot(p_{j,t}-d_{j,t})\forall i\in L,\quad t=1,2,\ldots N \tag{28}$$

$$\underline{l}_{i,t}\le\sum_{j\in E}SF_{i,j}\cdot(p_{j,t}-d_{j,t})\le\bar{l}_{i,t}\forall i\in L,\quad t=1,2,\ldots N \tag{29}$$

C. HEATING SYSTEM CONSTRAINTS

In the heating system, the heat node constraint is:

$$h_{i,t}=c_p m_{i,t}^{n}(T_{i,t}^{NS}-T_{i,t}^{NR})\forall i\in H,\quad t=1,2,\ldots N \tag{30}$$

In the heat supply network, for load nodes $T_{i,t}^{NS}=T_{i,t}^{S}$. For source nodes $T_{i,t}^{S}$ is calculated using (35), where $t=1,2,\ldots N$. In the heat return network, for load nodes $T_{i,t}^{R}$ is calculated using (36). For source nodes $T_{i,t}^{NR}=T_{i,t}^{R}$, where $t=1,2,\ldots N$.

The heat exchanger supply and return temperatures of node i at period t should satisfy:

$$\underline{T}_i^{NS}\le T_{i,t}^{NS}\le\bar{T}_i^{NS}\quad\forall i\in H,\quad t=1,2,\ldots N \tag{31}$$

$$\underline{T}_i^{NR}\le T_{i,t}^{NR}\le\bar{T}_i^{NR}\quad\forall i\in H,\quad t=1,2,\ldots N \tag{32}$$

Also, we have pipeline storage constraint:

$$\sum_{t=1}^{N}\left(\sum_{i\in H_G} h_{i,t}-\sum_{i\in H} h_{i,t}\right)\Delta t \geq 0 \tag{33}$$

Moreover, additional equality constraints are added to ensure heat power within each Δt_H is invariant:

$$h_{i,t}=h_{j,t}\forall i\in H,t,j\in W_k,\quad k=1,2,\ldots N_H \tag{34}$$

The node temperature mixing equations are:

$$\begin{aligned}&\left(m^n_{i\in H_G,t}+\sum_j m_{j,t}\right)T^S_{i,t}\\&=\left(m^n_{i\in H_G,t}T^{NS}_{i\in H_G,t}\right)+\left(\sum_j m_{j,t}\tau^{SO}_{j,t}\right)\\&\quad\forall i\in H, j\in P_S\cap In(i),\quad t=1,2,\ldots N\end{aligned} \tag{35}$$

$$\begin{aligned}&\left(m^n_{i\in H_L,t}+\sum_j m_{j,t}\right)T^R_{i,t}\\&=\left(m^n_{i\in H_L,t}T^{NR}_{i\in H_L,t}\right)+\left(\sum_j m_{j,t}\tau^{RO}_{j,t}\right)\\&\quad\forall i\in H, j\in P_R\cap In(i),\quad t=1,2,\ldots N\end{aligned} \tag{36}$$

The pipe inlet temperature equals the temperature of its connecting node:

$$\tau^{SI}_{j,t}=T^S_{i,t} j\in P_S\cap Lv(i), i\in H,\quad t=1,2,\ldots N \tag{37}$$

$$\tau^{RI}_{j,t}=T^R_{i,t} j\in P_R\cap Lv(i), i\in H,\quad t=1,2,\ldots N \tag{38}$$

The pipeline model equations are:

$$\tau'^{SO}_{i,t}=\sum_{k=t-\varphi_{i,t}}^{t-\gamma_{i,t}} K_{i,t,k}\tau^{SI}_{i,k}\forall i\in P_S,\quad t=1,2,\ldots N \tag{39}$$

$$\tau'^{RO}_{i,t}=\sum_{k=t-\varphi_{i,t}}^{t-\gamma_{i,t}} K_{i,t,k}\tau^{RI}_{i,k}\forall i\in P_R,\quad t=1,2,\ldots N \tag{40}$$

$$\begin{aligned}\tau^{SO}_{i,t}=T^a_{i,t}+(\tau'^{SO}_{i,t}-T^a_{i,t})\times\exp\left[-\frac{\lambda_i\Delta t_H}{A_i\rho c_p}\left(\gamma_{i,t}\right.\right.\\\left.\left.+\frac{1}{2}+\frac{S_{i,t}-R_{i,t}}{m_{i,t-\gamma_{i,t}}\Delta t_H}\right)\right]\forall i\in P_S,\quad t=1,2,\ldots N\end{aligned} \tag{41}$$

$$\begin{aligned}\tau^{RO}_{i,t}=T^a_{i,t}+(\tau'^{RO}_{i,t}-T^a_{i,t})\times\exp\left[-\frac{\lambda_i\Delta t_H}{A_i\rho c_p}\left(\gamma_{i,t}\right.\right.\\\left.\left.+\frac{1}{2}+\frac{S_{i,t}-R_{i,t}}{m_{i,t-\gamma_{i,t}}\Delta t_H}\right)\right]\forall i\in P_R,\quad t=1,2,\ldots N\end{aligned} \tag{42}$$

where $K_{i,t,k}$, $\varphi_{i,t}$, $\gamma_{i,t}$, $S_{i,t}$, and $R_{i,t}$ are calculated according to [17].

D. ENERGY SOURCES CONSTRAINTS

1) COMBINED HEAT AND POWER UNITS

In the identical model, the CHP constraints are:

$$B_{k,i}p^C_{i,t}+K_{k,i}h^C_{i,t}\leq v_{k,i}\forall i\in G,\quad t=1,2,\ldots N \tag{43}$$

$$B_{k,i}p^C_{i,t}+K_{k,i}h^C_{i,t}= v_{k,i}\forall i\in G,\quad t=1,2,\ldots N \tag{44}$$

The ramping constraints of CHP units are:

$$D_{e,i}\cdot\Delta t\leq p^C_{i,t}-p^C_{i,t-1}\leq U_{e,i}\cdot\Delta t\forall i\in G,\quad t=2,3,\ldots N \tag{45}$$

$$D_{h,i}\cdot\Delta t\leq h^C_{i,t}-h^C_{i,t-1}\leq U_{h,i}\cdot\Delta t\forall i\in G,\quad t=2,3,\ldots N \tag{46}$$

The supply temperature of the CHP unit must satisfy:

$$T^{NS}_{j,t}=T^{Set}_{i,t}\forall i\in G, j=\Gamma_G(i),\quad t=1,2,\ldots N \tag{47}$$

2) THERMAL GENERATOR AND MAIN GRID

The electric power outputs of the thermal generator and the main grid at source i must satisfy:

$$\begin{aligned}&\underline{p}^G_i\leq p^G_{i,t}\leq\bar{p}^G_i\quad\forall i\in G,\quad t=1,2,\ldots N\\&\underline{p}^T_i\leq p^T_{i,t}\leq\bar{p}^T_i\quad\forall i\in G,\quad t=1,2,\ldots N\end{aligned} \tag{48}$$

At the same time, the thermal generator must satisfy the ramping constraint (45).

IV. CASE STUDIES

The case studies address the following questions: 1) Do the two proposed asynchronous dispatch models produce the same solution? 2) Does the heat dispatch interval influence the results? 3) Is it necessary to use the asynchronous dispatch method since we already have the synchronous dispatch method?

The simulations are performed on a laptop with 2.80 GHz CPU and 16GB memory. Programs are coded using Matlab, and the toolbox YALMIP is used as a socket between Matlab and solvers CPLEX.

A. COMPARISON OF THE TWO ASYNCHRONOUS DISPATCH MODELS

This simulation addresses question 1: whether the hybrid model and the identical model produce the same solution. As shown in Fig. 5, the validation is based on a practical combined heat and power system in a city situated in Northeast China, which incorporates a 19-bus transmission-level electric power system and a 69-node heating system whose total pipeline length is about 90 km [27]. The system has 1 CHP unit at heat node 1 as well as 2 equivalent heat sources at heat node 37 and 67, respectively. For simplicity, the above 3 sources are named as CHP 1, CHP 2, and CHP 3, respectively.

In the economic dispatch, the electric dispatch interval is 15 minutes, and the heat dispatch interval is 60 minutes. Thus, in the hybrid model, $\Delta t_E=15$ min and $\Delta t_H=60$ min. In the identical model, $\Delta t=15$ min.

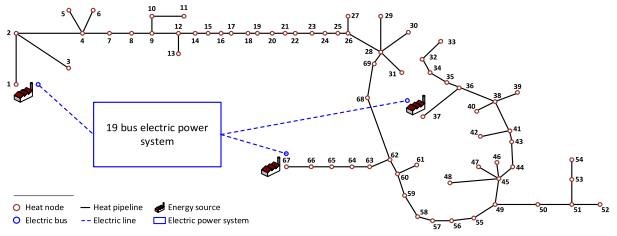

FIGURE 5. The structure of the combined heat and power system in a city in Northeast China.

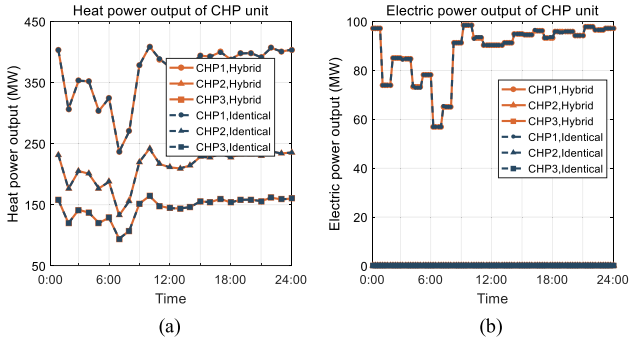

FIGURE 6. The (a) electric power and (b) heat power outputs of CHP units in the hybrid model and the identical model.

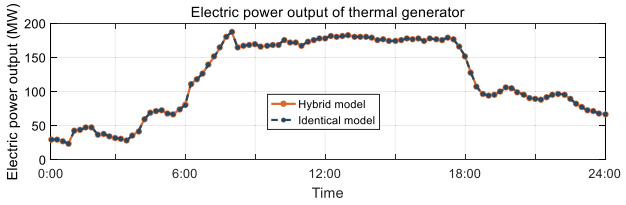

FIGURE 7. The electric power generated by the thermal generator.

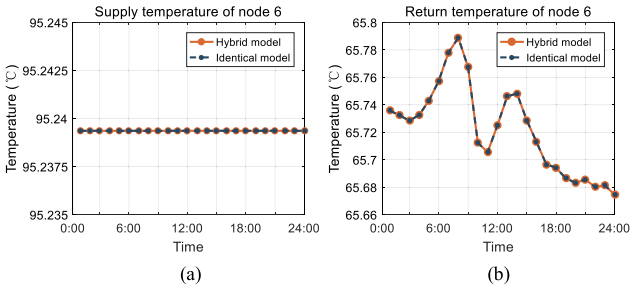

FIGURE 8. The node exchanger (a) supply temperature and (b) return temperature in the heating system.

TABLE 2. Computational efficiency of the hybrid model and the identical model.

Model	Hybrid model	Identical model
Overall cost ($)	6.72×10^5	6.72×10^5
Variable number	14946	54618
Total CPU time (s)	21.30	72.79
YALMIP time (s)	10.53	33.27
Solver time (s)	10.77	39.52

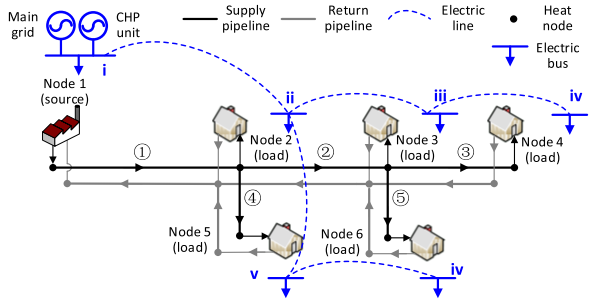

FIGURE 9. The topology of the test combined heat and power system.

Obviously, from the results shown from Fig. 6 to Fig. 8, the hybrid model and the identical model have the same solution. This phenomenon is more apparent in Fig. 8, where the supply and return temperatures at heat node 6 have no difference between the two asynchronous models. The reason is that the additional equality constraints in the identical model ensure the heat power outputs are invariant during each Δt_H.

If we look at Fig. 6 carefully, the back-pressure CHP unit at heat node 1 adjusts its electric and heat power outputs every 60 minutes even if it has the ability to adjust electric power every 15 minutes. This is caused by the linear relationship between electric and heat power outputs: the slow adjustment of heat power limits the fast adjustment ability of electric power. As a result, the fast-changing electric load is satisfied by the thermal generator as shown in Fig. 7 because the electricity price is higher compared with the cost of the thermal generator. This result illustrates in a combined heat and power system, although an electric-heat coupling device (here is the back-pressure CHP unit) has the fast adjustment ability for the electric variables, if the electric and heat power outputs are tightly coupled, the slow adjustment of heat variables may restrict its fast adjustment ability. Therefore, additional flexible electric sources are needed to maintain the electric supply-demand balance even if the capacities of electric-heat coupling devices are enough for the electric load.

The computational efficiency of the two methods is summarized in Table 2 where the YALMIP time indicates the CPU time consumed by YALMIP to upload the objective function and constraints, and the solver time indicates the CPU time consumed by the solver to solve the optimization program. The identical model consumes more CPU time than the hybrid model due to more constraints and decision variables.

B. PERFORMANCE UNDER DIFFERENT DISPATCH INTERVALS

This case addresses question 2: How the heat dispatch interval Δt_H influences the results of the asynchronous dispatch.

The simulations are based on the combined heat and power system in Fig. 9 [17], which incorporates a 6-bus electric power system and a 6-node heating system with a CHP unit

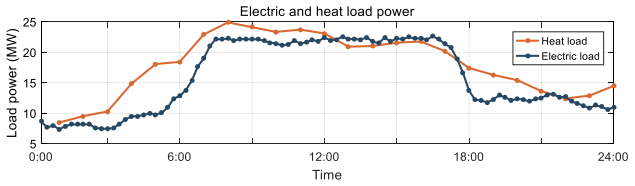

FIGURE 10. The sum of electric and heat loads of the test system.

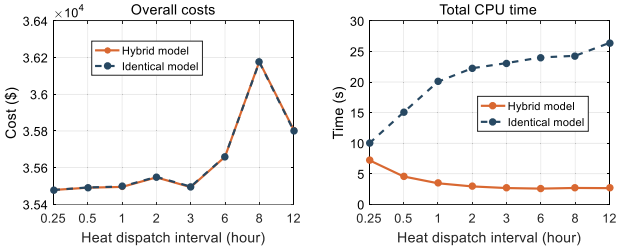

FIGURE 11. The (a) overall costs and (b) total CPU time under different Δt_H.

and a thermal generator. The power system can purchase electricity from the main grid through the tie-line. The sums of electric load and heat load are shown in the orange and blue curves in Fig. 10, respectively, where the load at node (bus) 3 is the residential load and the loads at other nodes (buses) are industrial loads. The dispatch intervals of the electric power system and the heating system are 15 minutes and 60 minutes, respectively.

As shown in Fig. 11 (a), when increasing the heat dispatch interval, Δt_H, the total generation cost experiences a slight increase ($<2\%$) because the adjustment flexibilities of CHP units and the heating network are restricted by the long heat dispatch intervals. Since the heat power within Δt_H may not be satisfied, the total costs decrease when $\Delta t_H = 3$ hour and $\Delta t_H = 12$hour. In brief, under given conditions, changing Δt_H under the given conditions will not have a significant influence on overall costs.

As shown in Fig. 11 (b) the CPU time of solving the hybrid model is much less than the identical model. With Δt_H increasing, the CPU time of the hybrid model is decreasing, while that of the identical model is increasing as a result of constraint numbers: The total dispatch time (24 hours) does not change when heat dispatch interval Δt_H is longer, so there are less heat constraints in the hybrid model but more constraints in the identical model due to adding more equality constraints. Thus, when Δt_H becomes longer, the computational efficiency of the hybrid model increases while that of the identical model decreases.

Moreover, this case simulation provides a supportive answer for question 1: under different Δt_H, the hybrid model has the same solution as the identical model. For example, in Fig. 12, the result of the exchanger supply temperature at heat node 6 clearly demonstrates that the temperatures calculated by the two asynchronous models are the same.

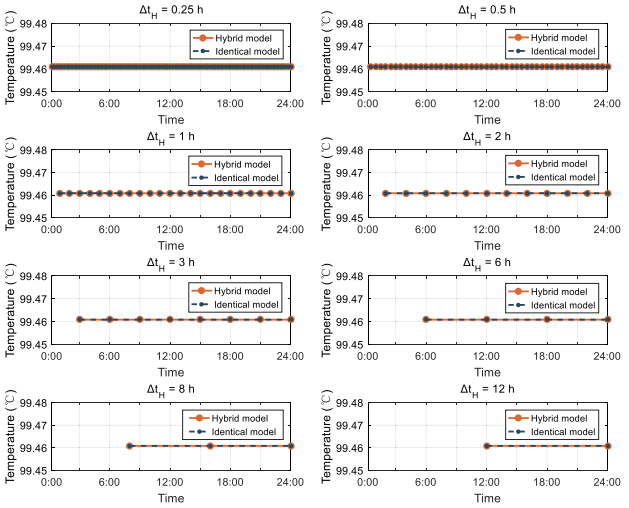

FIGURE 12. The node exchanger supply temperature of heat node 6 under different Δt_H.

C. NECESSITY OF USING ASYNCHRONOUS DISPATCH

Two cases are simulated to demonstrate the necessity of using the asynchronous dispatch method rather than the existing synchronous dispatch method, which ignores the different dispatch time scales of electricity and heat.

The simulations are based on the topology and data in Fig.9, where the dispatch intervals of the electric power system and the heating system are 15 minutes and 60 minutes, respectively. This setting means if a new dispatch command is not 60 minutes later in the heating system than the last dispatch command, it cannot be executed in practice because the heating system with large inertia cannot respond so fast.

1) COMPARISON WITH SYNCHRONOUS DISPATCH WITH HEAT DISPATCH TIME SCALE

In the synchronous method, one idea to deal with the different dispatch time scales of electricity and heat is to adopt a conservative manner: Let the electric power system follows the longer heat dispatch time scale, i.e., $\Delta t_S = 60$ min where Δt_S is the dispatch interval in the synchronous method. Thus, both the electric power system and the heating system can execute all dispatch commands.

On contrast, in the asynchronous method, $\Delta t_E = 15$ min and $\Delta t_H = 60$min. The key given conditions and results are summarized in Table 3: where the "total electric unbalanced energy" indicates the sum of the absolute value of electric unbalanced energy.

Under the above conditions, the asynchronous and synchronous methods all find the global optimums and successfully satisfy the heat loads. For example, heat power outputs and temperatures of the two dispatch methods have the same results as presented in Fig. 13 and Fig. 14, respectively.

However, as shown in Fig. 15 (a) and Table 3, the synchronous dispatch fails to satisfy the electric load: The power balance between the generation side and load side is not satisfied for 18 hours in a day, and the total unbalanced electric energy is 14.3MWh as presented in the grey block of Table 3.

TABLE 3. Comparison of asynchronous dispatch and synchronous dispatch under $\Delta t = 60$ min.

Methods	Asynchronous dispatch	Synchronous dispatch
Electric dispatch interval (min)	15	60
Heat dispatch interval (min)	60	60
Total electric load (MWh)	379.4	379.4
Total electric generation (MWh)	379.4	378.8
Total electric unbalanced energy (MWh)	0	14.3
Total heat load (MWh)	429.8	429.8
Total heat generation (MWh)	431.7	431.7

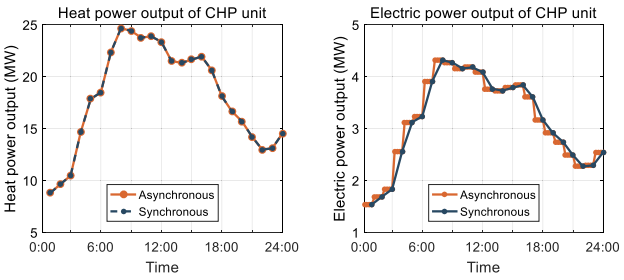

FIGURE 13. The (a) electric power and (b) heat power outputs of the CHP unit in asynchronous dispatch (asynchronous) and synchronous dispatch (synchronous).

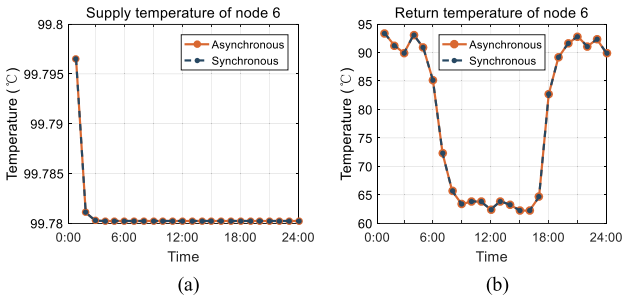

FIGURE 14. The node exchanger (a) supply temperature and (b) return temperature of node 6 in the heating system.

By calculating the electric power unbalance rate between the generation side and the load side $r = \left|\left(p_{i,t} - d_{i,t}\right)/d_{i,t}\right| \times 100\%$ and plotting it in Fig. 15 (b), we find the synchronous dispatch presents a large generation-load unbalance rate. For example, at 17:15, about 35% of electric load power is not satisfied, and at 3:15, 5:15, and 6:15, it has about 30% generation surplus. The reason for the synchronous dispatch's failure is that the dispatch interval Δt is so large that the electric load within Δt cannot be satisfied. Thus, in the day-ahead synchronous dispatch, selecting a dispatch interval Δt based on the heat dispatch time scale can lead to the break of the electric generation-load power balance. As a result, intraday dispatch and real-time dispatch have to give up the most

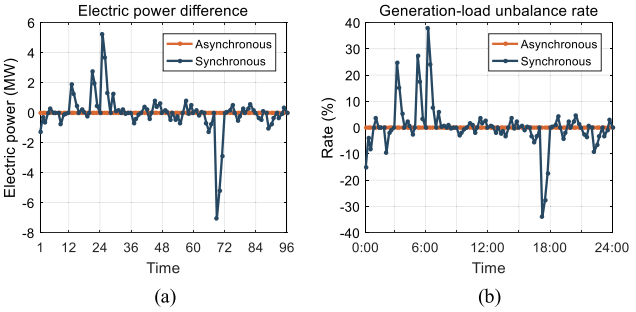

FIGURE 15. The (a) electric power difference and (b) electric power unbalance rate between the generation side and the load side.

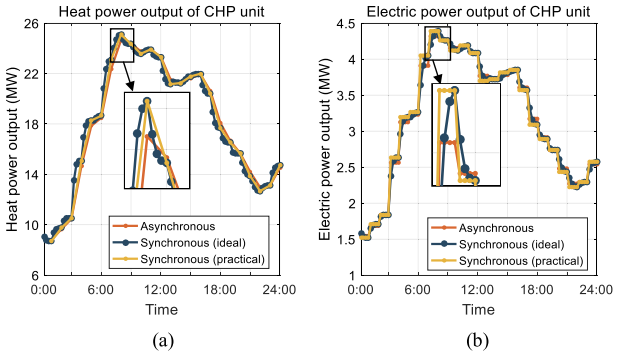

FIGURE 16. The (a) electric power and (b) heat power outputs of the CHP unit.

efficient plan to eliminate the unbalance power in the day-ahead dispatch. In contrast, the proposed asynchronous method can satisfy both electric and heat demands successfully without any violation as shown in the orange curves in Fig. 15.

In brief, compared to the synchronous method following the heat dispatch time scale, the proposed asynchronous method eliminates the electric generation-demand unbalance and improves system efficiency by allowing the electric power system follows its fast adjustment time scale.

2) COMPARISON WITH SYNCHRONOUS DISPATCH WITH ELECTRIC DISPATCH TIME SCALE

In the synchronous method, another idea of dealing with the different dispatch time scales is directly let the electric power system dominate the heating system, which indicates the heat dispatch time scale is required to follow the electric dispatch time scale. Thus, in this case, $\Delta t_S = 15$ mineven if the heating system cannot respond to the commands so fast. Under this condition, practically the heating system cannot execute all but a part of dispatch commands due to its large inertia.

As shown in Fig. 16, we can see three curves named Asynchronous, Synchronous (ideal), and Synchronous (practical) which are the abbreviations of the asynchronous method, synchronous method adjusting the heating system

TABLE 4. Comparison of the asynchronous method and the synchronous method under $\Delta t = 15$ min.

Methods	Asynchronous method	Synchronous (ideal)	Synchronous (practical)
Electric dispatch interval (min)	15	15	15
Heat dispatch interval (min)	60	15	60
Successfully solved	Yes	Yes	No

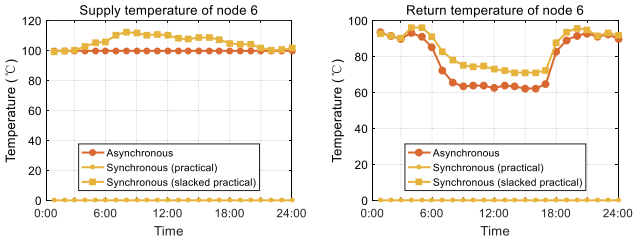

FIGURE 17. The node exchanger (a) supply temperature and (b) return temperature of node 6 in the heating system.

every 15 minutes, and synchronous method adjusting the heating system every 60 minutes in practice. More precisely, the result of Synchronous (practical) is a result of implementing Synchronous (ideal) in practice.

As shown in Table 4, both asynchronous dispatch and the Synchronous (ideal) find the global optimums while the Synchronous (practical) is an infeasible problem.

To study the infeasibility problem of the Synchronous (practical), we relax the optimization program by allowing the heat exchanger temperature limits and the CHP set temperature constraints to be broken. After that, the optimization program can be successfully solved, whose result is marked as "Synchronous (slacked practical)" in the yellow curves with blocks in Fig. 17. This result shows that if we let the fast electric power system dominate the heating system and directly implement the dispatch commands, the heat exchanger supply temperature is approaching 120°C as shown in Fig. 17 (a), which indicates the hot water becomes steam. As a result, the heat exchangers will not work at a normal state and probably have serious problems, which threatens the reliable operation of the heating system.

In contrast, as shown in the orange curves in Fig. 16 and 17, the asynchronous dispatch method can be successfully solved and implemented in practice with all constraints satisfied because the different dispatch time scales of the electric power system and the heating system are incorporated.

In brief, if we use the synchronous method and allow the electric power system to dominate the heating system in terms of dispatch time scale, the dispatch commands are infeasible to be executed in practice. This problem can be overcome by the proposed asynchronous method.

V. CONCLUSION

In this article, two asynchronous economic dispatch models, i.e., hybrid model and identical model, are proposed for combined heat and power systems to incorporate different dispatch time scale of electricity and heat. In the asynchronous dispatch, with the heat dispatch interval increasing, the total CPU time of the hybrid model is decreasing while that of the identical model is increasing, but the calculation results of the two models hold the same. From the comparisons in case studies, the existing synchronous dispatch method either has problems in efficiency due to leaving electric power unbalance to the next dispatch layer or becomes infeasible to implement in practice because of breaking security constraints. Therefore, it is essential to adopt the proposed asynchronous dispatch method when the electric power system and the heating system have different dispatch time scales.

Based on the proposed asynchronous dispatch method, there are some interesting directions open for future study. For example, how to determine the optimal dispatch intervals if we have multiple CHP units operating in parallel is a note-worthy topic. Moreover, how to implement the asynchronous dispatch in the background of electricity market is another important but challenging point.

APPENDIX

The appendix discusses two circumstances: 1) How to revise the identical model if k_E is not an integer? 2) How to dispatch multiple CHP units with different adjustment time scales?

A. SPECIAL DISPATCH INTERVALS

In the identical model formulated in Section III, we assume the heat dispatch interval is multiple of the electric dispatch interval, i.e., $\Delta t_H = k_E \cdot \Delta t_E = k_E \cdot \Delta t$. This assumption holds in most cases because in the day-ahead economic dispatch, the electric dispatch interval is 15 minutes, and the heat dispatch interval is in hours [4], [5]. However, in some special cases, this assumption is not satisfied. To deal with these special cases, we select the least common multiple Δt_{LMP} of Δt_E and Δt_H:

$$\Delta t_E = k_{LE} \cdot \Delta t_{LMP} \tag{49}$$

$$\Delta t_H = k_{LH} \cdot \Delta t_{LMP} \tag{50}$$

where k_{LE} and k_{LH} are integer coefficients. Then we let $\Delta t = \Delta t_{LMP}$ in the identical model and give equality constraints to guarantee the variables during each Δt_E and Δt_H are invariant. As a result, even if the Δt_H is not multiple of Δt_E, we can still realize the asynchronous dispatch.

B. MULTIPLE CHP UNITS WITH DIFFERENT ADJUSTMENT TIME SCALES

If a combined heat and power system has multiple CHP units with different adjustment scales, we can still use the method in Appendix A. First, let the dispatch interval in the identical model equals the least common multiple of the adjustment time scales of different CHP units. Second, give

equality constraints to ensure each CHP unit's electric and heat outputs are invariant during its own dispatch interval. By taking the two steps, the system operator can implement the asynchronous dispatch where different CHP units have different adjustment time scales.

REFERENCES

[1] J. Wu, J. Yan, and H. Jia, "Integrated energy systems," *Appl. Energy*, vol. 167, pp. 155–157, Mar. 2016. [Online]. Available: https://www.sciencedirect.com/science/article/pii/S0306261916302124?via%3Dihub

[2] P. Mancarella, "MES (multi-energy systems): An overview of concepts and evaluation models," *Energy*, vol. 65, pp. 1–17, Feb. 2014.

[3] H. Sun *et al.*, "Integrated energy management system: Concept, design, and demonstration in China," *IEEE Electrific. Mag.*, vol. 6, no. 2, pp. 42–50, Jun. 2018.

[4] H. Lund *et al.*, "4th generation district heating (4GDH): Integrating smart thermal grids into future sustainable energy systems," *Energy*, vol. 68, pp. 1–11, Apr. 2014.

[5] A. Benonysson, B. Bøhm, and H. F. Ravn, "Operational optimization in a district heating system," *Energy Convers. Manage.*, vol. 36, no. 5, pp. 297–314, May 1995.

[6] B. Deng *et al.*, "Optimal scheduling for combined district heating and power systems using subsidy strategies," *CSEE J. Power Energy Syst.*, vol. 5, no. 3, pp. 399–408, Sep. 2019.

[7] Y. Zhou, W. Hu, Y. Min, and Y. Dai, "Integrated power and heat dispatch considering available reserve of combined heat and power units," *IEEE Trans. Sustain. Energy*, vol. 10, no. 3, pp. 1300–1310, Jul. 2019.

[8] S. Huang, W. Tang, Q. Wu, and C. Li, "Network constrained economic dispatch of integrated heat and electricity systems through mixed integer conic programming," *Energy*, vol. 179, pp. 464–474, Jul. 2019.

[9] J. Hao *et al.*, "A heat current model for heat transfer/storage systems and its application in integrated analysis and optimization with power systems," *IEEE Trans. Sustain. Energy*, vol. 11, no. 1, pp. 175–184, Jan. 2020.

[10] M. Nazari-Heris, B. Mohammadi-Ivatloo, G. B. Gharehpetian, and M. Shahidehpour, "Robust short-term scheduling of integrated heat and power microgrids," *IEEE Syst. J.*, vol. 13, no. 3, pp. 3295–3303, Sep. 2019.

[11] Y. Zhou, M. Shahidehpour, Z. Wei, Z. Li, G. Sun, and S. Chen, "Distributionally robust co-optimization of energy and reserve for combined distribution networks of power and district heating," *IEEE Trans. Power Syst.*, vol. 35, no. 3, pp. 2388–2398, May 2020.

[12] Z. Pan, J. Wu, H. Sun, Q. Guo, and M. Abeysekera, "Quasi-dynamic interactions and security control of integrated electricity and heating systems in normal operations," *CSEE J. Power Energy Syst.*, vol. 5, no. 1, pp. 120–129, 2019.

[13] Z. Li, W. Wu, J. Wang, B. Zhang, and T. Zheng, "Transmission-constrained unit commitment considering combined electricity and district heating networks," *IEEE Trans. Sustain. Energy*, vol. 7, no. 2, pp. 480–492, Apr. 2016.

[14] C. Lin, W. Wu, B. Zhang, and Y. Sun, "Decentralized solution for combined heat and power dispatch through benders decomposition," *IEEE Trans. Sustain. Energy*, vol. 8, no. 4, pp. 1361–1372, Oct. 2017.

[15] J. Yang, N. Zhang, A. Botterud, and C. Kang, "On an equivalent representation of the dynamics in district heating networks for combined electricity-heat operation," *IEEE Trans. Power Syst.*, vol. 35, no. 1, pp. 560–570, Jan. 2020.

[16] W. Gu, J. Wang, S. Lu, Z. Luo, and C. Wu, "Optimal operation for integrated energy system considering thermal inertia of district heating network and buildings," *Appl. Energy*, vol. 199, pp. 234–246, Aug. 2017.

[17] Z. Li, W. Wu, M. Shahidehpour, J. Wang, and B. Zhang, "Combined heat and power dispatch considering pipeline energy storage of district heating network," *IEEE Trans. Sustain. Energy*, vol. 7, no. 1, pp. 12–22, Jan. 2016.

[18] Y. Chen, Q. Guo, H. Sun, Z. Li, Z. Pan, and W. Wu, "A water mass method and its application to integrated heat and electricity dispatch considering thermal inertias," *Energy*, vol. 181, pp. 840–852, Aug. 2019.

[19] S. Yao, W. Gu, S. Zhou, S. Lu, C. Wu, and G. Pan, "Hybrid timescale dispatch hierarchy for combined heat and power system considering the thermal inertia of heat sector," *IEEE Access*, vol. 6, pp. 63033–63044, 2018.

[20] L. X. Wang *et al.*, "Multi-time scale dynamic analysis of integrated energy systems: An individual-based model," *Appl. Energy*, vol. 237, pp. 848–861, Mar. 2019.

[21] N. Liu, J. Wang, and L. Wang, "Hybrid energy sharing for multiple microgrids in an integrated heat–electricity energy system," *IEEE Trans. Sustain. Energy*, vol. 10, no. 3, pp. 1139–1151, Jul. 2019.

[22] Z. Bao, Q. Zhou, Z. Yang, Q. Yang, L. Xu, and T. Wu, "A multi time-scale and multi energy-type coordinated microgrid scheduling solution—Part I: Model and methodology," *IEEE Trans. Power Syst.*, vol. 30, no. 5, pp. 2257–2266, Sep. 2015.

[23] B. Zhang, W. Wu, T. Zheng, and H. Sun, "Design of a multi-time scale coordinated active power dispatching system for accommodating large scale wind power penetration," *Autom. Electr. Power Syst.*, vol. 35, no. 1, pp. 1–6, 2011.

[24] W. Gu *et al.*, "Hybrid time-scale operation optimization of integrated energy system," (in Chinese), *Electr. Power Autom. Equip.*, vol. 39, no. 8, pp. 1–11, 2019.

[25] D. Wang *et al.*, "Optimal scheduling strategy of district integrated heat and power system with wind power and multiple energy stations considering thermal inertia of buildings under different heating regulation modes," *Appl. Energy*, vol. 240, pp. 341–358, Apr. 2019.

[26] R. Lahdelma and H. Hakonen, "An efficient linear programming algorithm for combined heat and power production," *Eur. J. Oper. Res.*, vol. 148, no. 1, pp. 141–151, Jul. 2003.

[27] X. Qin, X. Shen, Y. Guo, Z. Pan, Q. Guo, and H. Sun, "Combined electric and heat system testbeds for power flow analysis and economic dispatch," *CSEE J. Power Energy Syst.* 2020.